DESIGN OPTIMIZATION OF COMPOSITE WINGS FOR THE KARI-SUAV TILTROTOR AIRCRAFT CONSIDERING WHIRL FLUTTER STABILITY

Jae-Sang Park, Dept. of Aerospace Information Eng., Konkuk Univ., Hwayang-dong, Gwangjin-gu, Seoul 143-701, Korea
SungNam Jung, Dept. of Aerospace Information Eng., Konkuk Univ., Hwayang-dong, Gwangjin-gu, Seoul 143-701, Korea
Myeong-Kyu Lee, Smart UAV Development Center, Korea Aerospace Research Institute, 45 Eoeun-dong, Yuseong-gu, Daejeon 305-333, Korea
Jai-Moo Kim, Smart UAV Development Center, Korea Aerospace Research Institute, 45 Eoeun-dong, Yuseong-gu, Daejeon 305-333, Korea

Abstract

This paper constructs the design optimization framework for the composite wing of a tiltrotor aircraft based on the KARI (Korea Aerospace Research Institute) SUAV (Smart Unmanned Aerial Vehicle) TRS4 model. The present optimal design attempts to find the cross-section layout which minimizes the structural weight of a composite wing while satisfying a series of design constraints. The framework consists of various analysis and design tools that include a 2-D beam cross-section analysis, a whirl flutter analysis, and a 3-D strain/stress analysis under the worst wing-loading case. Variation of the wing sectional properties of tiltrotor aircrafts in the course of design optimization greatly affects the whirl flutter stability and exerts considerable influence on the structural integrity of the wing. In the framework, the whirl flutter stability is analyzed by the nonlinear flexible multibody analysis code DYMORE and the structural integrity is investigated using a MATLAB-based 3-D strain analysis module along with the previous load analysis result. MATLAB is used to conduct the optimization with a gradient-based optimizer and integrate all of the design and analysis tools. The nonlinear constraints associated with the aeroelastic stability and the structural integrity are also considered. For optimal design examples using the developed framework, a simplified cross-section model based on the KARI SUAV TRS4 composite wing is considered as an initial model. Design optimization examples are discussed to show the validity of the proposed framework and to illustrate the reduction of the structural weight of the composite wing. Through two examples, weight reductions of the wings of 26% and 40% are achieved while maintaining the whirl flutter stability margins.

1. INTRODUCTION

Tiltrotor aircrafts are capable of conducting versatile operations such as vertical take-offs and landings, hovering, and high-speed cruise flights. Tiltrotor aircraft have two wing-tip-mounted nacelle-rotor assemblies which can rotate to a vertical position in helicopter mode and to a horizontal position in airplane mode. Due to the dual functionality of the rotor, the rotor of this type of aircraft is often termed a proprotor. After research and development of nearly 50 years, tiltrotor aircraft went into full-scale productions such as the Bell/Boeing V-22 Osprey, the Bell Eagle Eye and the Bell/Agusta 609 emerged. In Korea, KARI (Korea Aerospace Research Institute) developed the SUAV (Smart Unmanned Aerial Vehicle [1]) based on the tiltrotor concept starting in 2002. This tiltrotor aircraft is shown in Figure 1, and its general properties are given in Table 1.

Due to the unique characteristics of tiltrotor aircraft, the wing-pylon-rotor system is the most critical and complicated component. The wing, pylon and rotor are mechanically connected to each other; therefore, their behaviors are tightly coupled. This makes the wing-pylon-rotor system design of a tiltrotor aircraft be a challenging task. Particularly when a tiltrotor aircraft flies in high-speed airplane mode, aeroelastic instability which is defined as a whirl flutter can occur. The whirl flutter stability is caused by coalescence of rotor-produced aerodynamic forces and wing elastic modes. Johnson [2] developed a comprehensive mathematical model based on a rigid/linear-blade theory for whirl flutter analyses. Howard [3] studied the aeromechanical instability of tiltrotor aircraft with soft-in-plane rotors, which are prone to ground and air resonance problems. Hathaway [4] applied both active and passive techniques to enhance the whirl flutter stability margins of tiltrotors. These approaches [2-4] used rigid blades and elastic wings for simplicity and efficiency of the comprehensive aeroelastic analysis. Nixon [5] studied the aeromechanical behavior of tiltrotor aircrafts using a nonlinear and elastically coupled composite beam model. Recently, the aeromechanics of tiltrotor aircrafts were investigated [6-8] by nonlinear flexible

multibody dynamics analysis tools such as MBDYN [9] and DYMORE [10]. Although multibody dynamics analyses require a considerable amount of computing resource, they can elaborately describe rotor control systems such as pitchlinks, pitch horns, and swashplates as well as complicated conversion components and lead-lag dampers. These analyses can determine the key variables crucial to the aeromechanics behavior of tiltrotor aircrafts.

From the previous investigations, the wing sectional properties as well as the proprotor properties are known to have a significant influence on the whirl flutter stability. In particular, the flapwise bending and torsion stiffness of a wing largely affects the whirl flutter stability [5]. In the references [11, 12], the composite wing design of a tiltrotor aircraft was accomplished through the use of the elastic tailoring concept of the composites. An airfoil with a thickness ratio of 23% was initially used as the reference (metal) wings of the tiltrotor aircraft for the provision of high torsional stiffness. The elastic tailoring of composite materials leads to a reduction in the wing thickness ratio from 23% to 18% while satisfying the requirements of stability and strength without additional weight. The thinner airfoil reduces the drag, increases the maximum speed, and thus improves the overall performance of the tiltrotor aircraft.

It is desirable that the structural weight of a wing is minimized so as to hold more fuel and maximize internal/external storage unless aeroelastic instability and structural failure will result. Therefore, the present work attempts to minimize the structural weight of a composite wing of a tiltrotor aircraft based on the KARI SUAV. Two level studies are carried out. First, whirl flutter stability, which is one of the critical design constraints, is investigated as the properties of the wing sections are varied in order to understand the effect of these properties on the whirl flutter stability. DYMORE, a nonlinear flexible multibody dynamics analysis code, is utilized to investigate the whirl flutter stability of a semi-span model. This parameter study can provide a design guideline for efforts to reduce the structural weight of a composite wing while maintaining whirl flutter stability margin. Second, a design optimization framework is constructed to minimize the structural weight of a composite wing. The optimization framework finds the cross-section layout of a composite wing which minimizes the structural weight while satisfying a series of design constraints. These requirements are associated with the locations of the center of gravity and the elastic axis, the damping value of the wing beam mode, and the wing strength based on local 3-D stress and strain fields under the worst loading conditions. For the current framework, the UM/VABS (University of Michigan/Variational-Asymptotic Beam Cross-Sectional Analysis [13]) - a 2-D beam cross-section analysis tool for a composite wing, DYMORE for the whirl flutter stability investigation, and a 3-D stress/strain analysis code for the structural integrity analysis are integrated with a gradient-based optimizer [14]. MATLAB integrates all of the design and analysis tools and carries out the design optimization. The result shows that the wing weight is reduced significantly through the design optimization while all design constraints are satisfied.

2. DESIGN OPTIMIZATION FRAMEWORK AND TILTROTOR MULTIBODY MODELING

2.1. Design optimization framework

A basic optimization problem is defined as

$$\begin{aligned} &\text{Minimize} \quad m = m(\mathbf{x}) \\ &\text{subject to} \\ &g(\mathbf{x}) \le \mathbf{0} \\ &\mathbf{x}_l \le \mathbf{x} \le \mathbf{x}_u \end{aligned} \tag{1}$$

where m is an objective function which is the structural weight or mass per unit length of a tiltrotor composite wing and $\mathbf{x}$ is a design variable vector which has a lower bound $\mathbf{x}_l$ and an upper bound $\mathbf{x}_u$.

Figure 2 shows an example of the cross-section configuration of a tiltrotor aircraft composite wing. Since nonstructural components such as the fuel, rotor-drive system and other components should be included inside of the wing structure of a tiltrotor aircraft, it is desirable that the geometric configuration of the spar be maintained or changed at least through design optimization to the extent possible. Hence, the ply thicknesses and the front web location may be selected as design variables to reduce the structural weight of a composite wing. The rear web location is not considered as a design variable because a change of the rear web location results in a change of the chord length of the flaperon which is located beyond the rear web.

Regarding the nonlinear constraints $g(\mathbf{x})$, the chordwise locations of the cross-sectional center of gravity (C.G.) and of the elastic axis (E.A.), the wing beam mode damping, and the maximum allowable wing local strain under the worst-case loading condition are implemented. Other constraints are also added to consider a feasible design.

The present design optimization framework consists of various numerical analysis components, as shown in Figure 3. MATLAB provides an environment to integrate all of these analysis elements and conducts a mathematical optimization. There are three important analysis elements that are

included.

First, UM/VABS [13] is used for a 2-D linear beam cross-section analysis of a composite wing. UM/VABS is a finite-element-based analysis tool which calculates the sectional stiffness, the inertia matrices of the beam and the actuation force/moment vectors of the active materials. In addition, it determines the chordwise-locations of the center of gravity, the elastic axis and the centroid. The sectional properties obtained by UM/VABS are transferred to DYMORE for the multibody modeling of the tiltrotor aircraft. UM/VABS utilizes the finite element method; therefore, it requires a cross-section mesh generator [15] which uses the input parameters to generate the finite element mesh. Although UM/VABS can analyze any type of cross-sectional configuration with or without internal structures, the mesh generator considers only the outer walls and webs.

Second, the nonlinear flexible multibody dynamics analysis code DYMORE is introduced to investigate the whirl flutter stability. DYMORE uses the geometrically exact beam theory [16] which has two slight modifications from the original formulation in its application to a flexible multibody dynamic system with arbitrary topology. The first is that the reference beam coordinate is a single inertial Cartesian coordinate instead of a moving and deformed coordinate. The second is that a displacement-based formulation is used instead of a mixed formulation. For the aerodynamic loads on the rotor blade, the lifting line theory with a finite-state dynamic inflow model [17] is included. Detailed DYMORE modeling of the semi-span model will be given in the next section.

Finally, a MATLAB-based 3-D stress/strain analysis module is applied in order to consider the structural integrity of the wing. This element computes the internal local 3-D strain and stress fields under the worst-case loading condition. The worst loading condition consists of the sectional wing loads for the flapwise bending and torsion moments from the previous load analysis [18] by ARGON [19]. The envelopes for the flapwise bending and torsion moments are shown in Figure 4. A sophisticated aeroelastic analysis should be conducted at each design iteration step to predict the airloads and structural loads on the wing precisely for various flight conditions. However, to reduce the computing time, the present 3-D stress/strain analysis uses the previous load analysis results of the KARI SUAV TRS4 wing model directly at every design step. In addition, a safety factor of 1.5 is considered. The previous load analysis results are used along with the information provided by UM/VABS to recover the local strain components at all points on the wing. The maximum strain criterion is applied for each component in the resulting strain and it is compared with the allowable values for the local constituent material.

As a mathematical optimization algorithm, the gradient-based constrained optimizer of the 'fmincon' command provided in MATLAB Optimization Toolbox [14] is integrated with the aforementioned analysis tools. This optimizer attempts to find a constrained minimum of a scalar function composed of several variables starting with an initial estimate. This is generally referred to as constrained nonlinear optimization. For a medium-scale optimization problem, the 'fmincon' function uses a Sequential Quadratic Programming (SQP) method. Based on that method, the present command solves a Quadratic Programming (QP) sub-problem at each iteration step. An estimate for the Hessian of the Lagrangian is updated with each iteration step using the BFGS formula [20]. Three types of termination criteria are provided: the maximum number of iterations, the tolerance of the design variables, and the tolerance of the function value. When one of these termination criteria is satisfied, the optimization iteration will be finished.

2.2. Multibody modeling of the KARI SUAV tiltrotor aircraft

As previously stated, DYMORE is used to investigate the whirl flutter stability. DYMORE has various multibody element libraries of rigid/elastic joints, rigid bodies and elastic bodies such as beams, plates and shells. The location, orientation and connections of these multibody elements should be specified to construct a complete DYMORE model. This powerful multibody modeling capability based on an arbitrary topology allows for highly realistic modeling of rotorcrafts; however, it requires tremendous effort to construct a completely new multibody model. This difficulty may be alleviated by starting the modeling from similar existing models. Therefore, this work uses a previously constructed DYMORE model from a previous study [7] and modifies it so that it is suitable for the semi-span model and to be executed in a newer version.

For symmetric modes in the airplane mode, the semi-span model including the rotor blades, pitch links, swashplates, pylon, hydraulic control actuators in the pylon and an elastic wing with the semi-span length is considered, as shown in Figure 5. The KARI SUAV uses a three-blade, stiff in-plane and gimbaled rotor system. A detailed view of its DYMORE modeling is given in Figure 6. The rotor blades are modeled as nonlinear elastic beams considering the coupled flap, lead-lag and torsion behaviors. The rotor blade consists of flexures, spindles, and outer blades whose sectional properties are provided by KARI. Each blade is discretized into 10 finite elements with the third-order polynomials. Three blades are joined at the hub which is modeled as a rigid body with joints for the prescribed rotation and gimbal motion.

Sophisticated rotor control system modeling is introduced. The pitch horns and the swashplates are modeled as rigid bodies, and a pitch link with a linear spring is considered to give the control system some flexibility. The relationship between the swashplate movement and the collective pitch angle is nonlinear, unlike in general helicopters; hence, swashplate movement based on the KARI test results is prescribed. The pylon is modeled as an elastic beam with rigid sectional properties and the pylon conversion actuator is modeled as a flexible joint consisting of a set of concentrated springs and dampers. The semi-span wing is considered as an elastic beam with 20 finite elements with the third-order polynomials. In the validation study of the whirl flutter stability analysis discussed in Section 3.1, the original wing sectional properties of the KARI TRS4 model are used. However, the sectional properties are updated through the design optimization process in the optimal design study. A wing is clamped to the fuselage which is modeled as a rigid body.

For the aerodynamic loads on the proprotor, the finite-state dynamic inflow model is used. This model is constructed by applying the acceleration potential theory to a rotor aerodynamics problem with a skewed cylindrical wake. More specifically, the induced flow at the rotor disk was expanded in terms of its modal functions. As a result, a three-dimensional, unsteady induced-flow aerodynamics model with a finite number of states is derived in the time domain. This model is an intermediate level of wake representation between the simplest momentum and the most complicated freewake methodologies. Furthermore, the aerodynamic interaction between the rotor and the wing is not considered for the simplicity of analysis.

Since DYMORE conducts the time domain analysis, a virtual experiment using the same procedure as a whirl flutter test in a wind tunnel can be realized. First, the proprotor is trimmed to obtain a windmilling condition which is a flight condition that is critical to whirl flutter stability. For a given airspeed and rotor rotational speed, the collective pitch is adjusted through the movement of the swashplate in order to obtain zero torque on the drive shaft. Second, the wing is excited to investigate the wing beam mode which has been well known as the most critical mode for the whirl flutter stability [5]. The wing tip is deflected with the appropriate time schedule for the excitation of the wing. Third, the free decay of the transient response is calculated to obtain the damping value. DYMORE uses Prony's method to predict the damping ratio. Finally, these procedures are repeated until the airspeed reaches the maximum flight speed.

3. NUMERICAL RESULTS

3.1. Validation and parameter studies of whirl flutter analysis

In this subsection, the DYMORE modeling of the whirl flutter analysis of the KARI SUAV TRS4 model is validated. The frequency and damping value of the wing beam mode in the airplane mode with a rotor speed of 1284 RPM are investigated in the airspeed range of 75 to 350 kts and the result is compared with the previous result [7]. The present result is obtained by the 2007 version of DYMORE while the reference result was predicted by version of DYMORE released in 2005. In addition, the wing beam mode damping and frequency in the aforementioned study [7] are calculated for an airspeed ranging from 75 to 325 kts. Hence, the frequency and damping values at 350 kts in the reference are extrapolated. Figure 7(a) shows the wing beam mode frequency. The present result clearly shows excellent agreement with the previous prediction. The wing beam mode frequency is decreased monotonically as the airspeed is increased from 75 kts. The wing beam mode damping is also given in Figure 7(b). The damping variation in the present study is similar to the damping in the referenced study [7]; however, two differences exist. First, although both damping predictions are increased as the airspeed is increased from 75 kts, the present damping result drops at 325 kts while the previous damping prediction falls at 300 kts. Second, the damping by DYMORE (2007) is over-predicted as compared with the result by the 2005 version of DYMORE. At this time, the prediction accuracy between the two results cannot be evaluated because there are no available experimental data for the whirl flutter test of the KARI SUAV. However, since DYMORE is still under development, changes or modifications of the algorithms for the stability analysis between two DYMORE versions may exist, which leads the difference in the damping predictions. As shown in Figure 7, whirl flutter instability is not observed because wing beam mode damping is positive in the entire airspeed region.

Following the validation study, the whirl flutter stability characteristics are investigated when the wing sectional properties are changed. However, all the properties of the proprotor are maintained as the original values. To change the properties of the wing sections, some scaling factors are applied to the baseline properties along the entire semi-span wing. This parameter study may serve as a basic guideline to reduce the structural weight of a composite wing without causing whirl flutter instability. Figure 8 shows the variation of the wing beam mode damping when the flapwise bending stiffness of a composite wing is changed. The variations of the wing flapwise bending stiffness are considered as 0.5 and 1.5 times the baseline properties. When a damping value of 350 kts is considered, although the wing flapwise bending stiffness is increased by 50% as

compared with the baseline stiffness, the damping value is quite similar to the baseline damping value. However, when the wing flapwise bending stiffness is decreased by 50%, the damping value is increased dramatically by 41%. This example shows that some composite plies related to the wing flapwise bending stiffness may be eliminated or that their thicknesses can be reduced appropriately to reduce the structural weight of a composite wing design. This will not lead to whirl flutter instability.

Figure 9 shows the variation of the wing beam mode damping when the inertial properties of the mass per unit length and inertia moments are varied from 0.5 to 1.5 times the baseline properties. This figure shows that the change of the wing inertia properties does not have a significant effect on the whirl flutter stability characteristics. Therefore, reducing the weight of a composite wing can be achieved while maintaining the whirl flutter stability margins.

Finally, the effect of the wing torsional stiffness is given in Figure 10. Unlike the previous example for the inertial property change, the torsional stiffness has a tremendous effect on the beam damping in the high-speed region. When 1.5 times the baseline torsional stiffness is used, the damping value is increased monotonically until the airspeed reaches 350 kts at which point the damping value is higher by 20% as compared with the baseline damping value. However, if the wing torsional stiffness is reduced by 50%, the damping is reduced dramatically above 250 kts. In particular, the wing beam mode damping at 350 kts is lower than the baseline damping value by 85% and will go to zero or have a negative value above 350 kts, which may cause whirl flutter instability. Therefore, the wing torsional stiffness should be maintained appropriately so as not to cause the whirl flutter phenomena when the weight reduction technique is applied to the composite wing of a tiltrotor aircraft.

The parameter study results suggest that the design optimization may work to reduce the structural weight of a tiltrotor composite wing by eliminating some composite plies associated with the flapwise bending stiffness or reducing their thickness appropriately while maintaining the plies related to the torsional stiffness. This weight reduction technique may not cause whirl flutter instability.

3.2. Modeling of a tiltrotor composite wing cross-section

For simplicity, a simplified composite wing cross-section is proposed as an initial model for the present design optimization examples rather than the original wing cross-section model of the KARI SUAV TRS4. The proposed wing model has an external shape identical to that of the original but has a simplified composite layup configuration. The airfoil of NACA64621 with a chord length of 0.8 m is used along the entire semi-span of a composite wing. In the modeling of the wing cross-section, only the skin, spar and web structures are considered; the flaperon beyond the rear web is not included, as shown in Figure 11. Carbon fabric prepregs are used. The relevant material properties are given in Table 2. Two types of carbon fabric were used; the first is a [0 90] fabric layer and the second is a [45 -45] fabric layer. A fiber angle of 0 degrees is coincident with the wing span axis. Four and nine fabric layers are used for the skin and spar/web structures, respectively. Their layup conditions are shown in Table 3.

Table 4 compares the sectional properties of the proposed wing to those at the 75% span location of the original wing. The sectional properties of the simplified wing model are clearly similar to those of the original wing model, although the torsional stiffness is somewhat higher than in the original. Figure 12 compares the whirl flutter stability of the semi-span model using the simplified wing and that when using the original wing. Both models use the original properties of the proprotor of the KARI TRS4 model. The proposed sectional properties given in Table 4 are used along the entire semi-span. The inertial properties of nonstructural components are not considered for the proposed wing modeling. As described previously, the higher the torsional stiffness becomes, the more stable the whirl flutter mode is. Hence, the proposed model is more stable compared to the original model. However, the whirl flutter stability characteristics with the proposed wing model are not quite different from those of the original model. Hence, the proposed wing properties can be used as an initial model in the design optimization study to reduce the structural wing weight.

3.3. Design optimization study

3.3.1. Case 1 design optimization

To maintain the geometric configuration of the spar of a composite wing, the thicknesses of two types of carbon fabric are selected as design variables in the Case 1 study. Hence, the locations of the front and rear webs are fixed. The ply thickness parameter t_k is introduced to change the thicknesses of the carbon fabric, and its meaning is a multiplier of the nominal thickness. Table 5 defines the optimization problem for Case 1. The constraints for the locations of the center of gravity and the elastic axis are related closely to the aeroelastic stability. The values of the wing beam mode damping and the local strain under the worst loading case are related with the constraints of the whirl flutter stability and structural integrity, respectively. The initial values for the two ply thickness parameters are assumed to be 1.0.

Figure 13 shows the convergence history of an

objective function which is the structural weight of a composite wing. A total of nine iterations were required to acquire a converged solution. Through the present optimal design, the structural weight of a composite wing is reduced significantly. The reduction is approximately 26%.

Figure 14 presents the convergence history of the ply thickness parameters. As shown in the figure, the thickness of the [45 -45] fabric remains very close to the original thickness, whereas the ply thickness parameter of the [0 90] fabric is converged to around the lower bound. Therefore, it can be expected that a reduction of the structural weight may be achieved by eliminating some [0 90] fabric layers or by reducing their thickness appropriately. As the [0 90] and [45 -45] fabrics are related to the flapwise bending stiffness and the torsional stiffness of a composite wing, respectively, the design optimization result reduces the flapwise bending stiffness and maintains the torsional stiffness of a composite wing, as shown in Figure 15. The torsional stiffness does not vary much during the design iteration procedure, whereas the other stiffness values of the axial stiffness, flapwise bending stiffness and chordwise bending stiffness are reduced from the initial values.

Figure 16 shows the variation of the wing beam mode damping at 350 kts in the airplane mode during the design iterations. Since the flapwise bending stiffness is reduced and the torsional stiffness does not change significantly relative to its initial value as given in Figure 15, the whirl flutter stability increases moderately.

3.3.2. Case 2 design optimization

The additional design variable, the location of the front web and two ply thickness parameters are considered in the Case 2 study. However, since a change in the location of the front web can alter the configuration of the wing spar structure, the upper boundary should be considered to avoid the extreme changes of the spar configuration. The definition of an optimization problem for Case 2 is given in Table 6. Particularly, for the ply thickness parameters in Case 2, the lower bound is reduced to 0.2 to obtain a more significant reduction of the structural wing weight.

Figure 17 presents the convergence history of the structural weight of a composite wing in Case 2. The figure shows that the number of iterations for the converged solution is 20 in Case 2. As compared with the Case 1 study, much more iteration attempts are conducted. As a result, the structural weight is reduced by approximately 40%, which corresponds to 1.38 times the result in Case 1.

The convergence history of the ply thickness parameters is given in Figure 18. Although the ply thickness parameter for the [45 -45] fabric shows a slight increase, the converged thickness is similar to the original thickness. As in the result of Case 1, the ply thickness parameter for the [0 90] fabric is converged to the lower bound which is assumed to be 0.2 in Case 2. Hence, it is expected that the variation in both the sectional stiffness and the wing beam mode damping value will be similar to the results in Case 1.

Figure 19 shows the variation of the front web location during the design optimization process. The location of the front web moved backward by 3.8% of the chord length. This result may be considered as reasonable given the insignificant amount of movement of the front web location, which will not cause significant reduction in the spar area for fuel or rotor-drive components.

The convergence history of the wing sectional properties is shown in Figure 20. Though the torsional stiffness is reduced by 18%, which is due to the backward movement of the front web location, this is not a great reduction. However, the flapwise bending stiffness is reduced dramatically by 53% after convergence. As compared with the obtained wing in Case 1, the designed wing in Case 2 is more flexible because the sectional properties in Case 2 are somewhat lower than those in Case 1.

Figure 21 shows the convergence history of the wing beam mode damping value at 350 kts in the airplane mode. As in the previous Case 1, the damping value increases given the considerable reduction in the flapwise bending stiffness. The converged wing beam mode damping in Case 2 is higher by approximately 30% compared to that in Case 1. Therefore, the optimization process in Case 2 designs a composite wing of a tiltrotor aircraft to be both lighter and more stable compared to that of Case 1.

4. CONCLUSION

In this work, a design optimization framework is constructed to minimize the structural weight of a tiltrotor composite wing. The framework consists of various analysis and design tools including a 2-D beam cross-section analysis, a nonlinear flexible multibody dynamic analysis for the investigation of the whirl flutter stability, and a 3-D strain/stress analysis under the worst loading case. MATLAB is used to integrate all of the analysis and design modules and to formulate the optimal design using a gradient-based optimizer. To obtain feasible design results, various design constraints related to the aeroelastic stability and the structural integrity are considered. Before the design optimization is conducted, a parameter study using the wing sectional properties of the KARI SUAV tiltrotor aircraft is carried out. The results show that when the wing flapwise bending stiffness is lower and the wing torsion stiffness is higher, the whirl flutter mode

becomes more stable. In addition, variation of the wing inertia properties does not affect the whirl flutter stability significantly. Two design optimization examples are discussed to minimize the structural weight of a composite wing of the tiltrotor aircraft based on the KARI SUAV. The first and second optimization studies show significant weight reductions of approximately 26% and 40%, respectively, with a moderate increase in the whirl flutter stability margin. These wing weight reductions are achieved through either eliminating some fabric plies for the flapwise bending stiffness in the composite wing or reducing their thickness. However the thickness of the fabrics for the torsional stiffness is maintained and the front web location is moved backward slightly. However, since the gradient-based optimizer used in this paper cannot guarantee the global minimum, another optimizer such as a Genetic Algorithm (GA) which can determine the global minimum will be introduced in the design framework in the future study.

ACKNOWLEDGEMENT

This work was supported by Brain Korea 21 in 2009, the Korea Foundation for International Cooperation of Science & Technology(KICOS) through a grant provided by the Korean Ministry of Education, Science & Technology(MEST) in 2009 (No. K20601000001) and the Korea Research Foundation (KRF) grant funded by the Korean government (MEST) in 2009 (2009-0075138). In addition, the authors would like to express their acknowledgements to Dr. Jinwei Shen at National Institute of Aerospace (NIA) and Dr. Bauchau at Georgia Institute Technology for giving valuable help to this work.

REFERENCES

[1] Choi S-W, Kang Y-S, Chang S-H, Koo S-O, Kim J-M. Small tiltrotor UAV development and conversion flight test. In: Proceedings of the 34th European Rotorcraft Forum; 2008.

[2] Johnson W. Dynamics of tilting proprotor aircraft in cruise flight. NASA Technical Note NASA TN D-7677 National Aeronautics and Space Administration; 1974.

[3] Howard AKT. The aeromechanical stability of soft-inplane tiltrotors. PhD Thesis. Department of Aerospace Engineering, The Pennsylvania State University; 2001.

[4] Hathaway EL. Active and passive techniques for tiltrotor aeroelastic stability augmentation. PhD Thesis. Department of Aerospace Engineering, The Pennsylvania State University; 2005.

[5] Nixon MW. Aeroelastic response and stability of tiltrotors with elastically coupled composite rotor blades. PhD Thesis. Department of Aerospace Engineering, The University of Maryland; 1993.

[6] Masarati P, Piatak DJ, Singleton JD, Quaranta G. Further results of soft-inplane tiltrotor aeromechanics investigation using two multibody analyses. In: Proceedings of the 60th American Helicopter Society Forum; 2004.

[7] Floros MW, Shen J, Lee M-K, Hwang S-J. Loads and stability analysis of an unmanned tilt rotor. In: Proceedings of the 62nd American Helicopter Society Forum; 2006.

[8] Shen J, Masarti P, Roget B, Piatak DJ, Nixon MK, Singleton JD. Stiff-inplane tiltrotor aeromechanics investigation using two multibody analyses. In: Proceedings of Multibody Dynamics 2007; 2007.

[9] Paolo M. MBDYN: http://www.aero.polimi.it/~mbdyn

[10] Baucahu OA. DYMORE Users' Manual: http://www.ae.gatech.edu/people/obauchau/Dwnld/dymore20/DymoreManual.pdf

[11] Brunson SL, Rais-Rohani M. A thin tailored composite wing box for a civil tiltrotor transport aircraft. In: Proceedings of the 37th AIAA/ASME/ASCE/AHS/ASC Structures, Structural Dynamics, and Materials Conference and Exhibit; 1996.

[12] Nixon MW, Piatak DJ, Corso LM, Popelka DA. Aeroelastic tailoring for stability augmentation and performance enhancement of tiltrotor aircraft. In: Proceedings of the 55th American Helicopter Society Forum; 1999.

[13] Cesnik CES, Palacios R. Modeling Piezocomposite Actuators Embedded in Slender Structures. In: Proceedings of 44th AIAA/ASME/ASCE/AHS/ASC Structures, Structural Dynamics and Materials Conference; 2003.

[14] Coleman TF, Zhang Y. Optimization Toolbox for Use with MATLAB. The MathWorks Inc., 1999.

[15] Brown EL. Integrated Strain Actuation in Aircraft with Highly Flexible Composite Wings. PhD Thesis, Department of Aeronautics and Astronautics, Massachusetts Institute of Technology; 2003.

[16] Hodges DH. A mixed variational formulation based on exact intrinsic equations for dynamics of moving beams. International Journal of Solids and Structures, 1990; 26(11):1253-73

[17] Peters DA, He CJ. Finite State Induced Flow Models Part II: Three-Dimensional Rotor Disk. Journal of Aircraft, 1995; 32(2): 323-333.

[18] Shin J-W, Kim S-C, Hwang, I-H. Loads Analysis of Smart UAV Using ARGON. Journal of the Korean Society for Aeronautical and Space Sciences 2005; 33(7): 76-84.

[19] Anonymous. ARGON: Multidisciplinary analytical support of aircraft design. Central Aerohydrodynamics Institute; 1991.

[20] Rao SS. Engineering Optimization: Theory and Practice. John Wiley & Sons, Inc., 1996.

Figure 1 Mock-up for the KARI SUAV

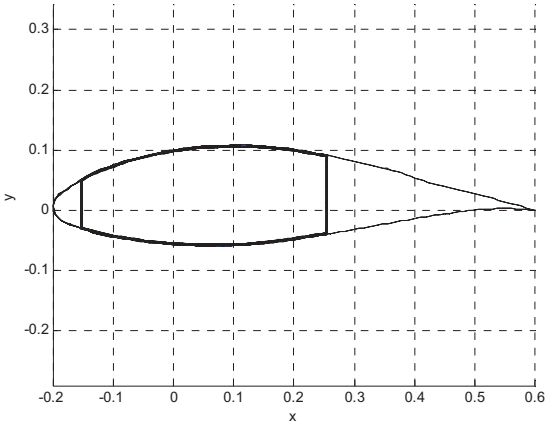

Figure 2 Cross-section configuration of a composite wing of the tiltrotor aircraft

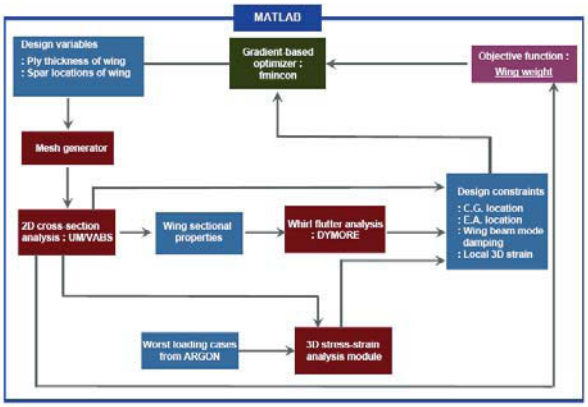

Figure 3 Design optimization framework

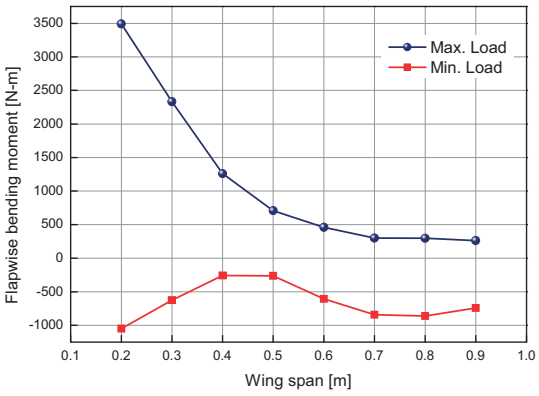

(a) Envelope of flapwise bending moment

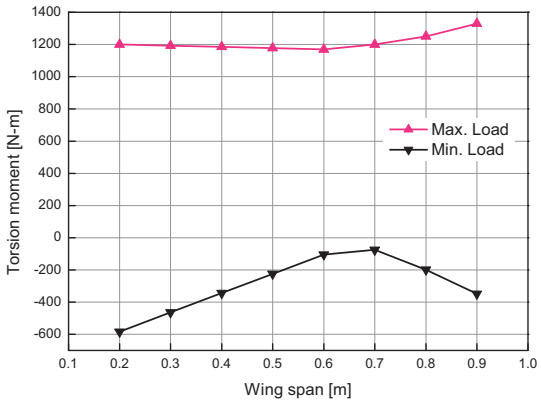

(b) Envelope of torsion moment

Figure 4 Envelopes of flapwise bending and torsion moments [18]

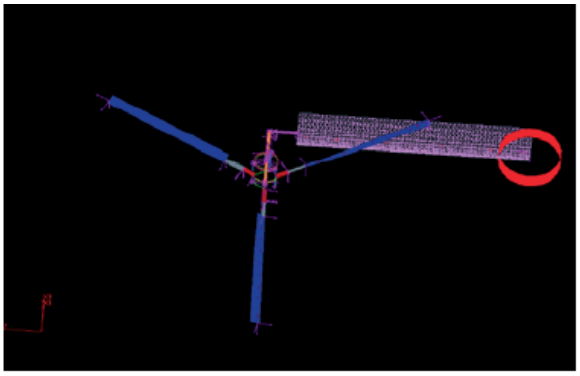

Figure 5 DYMORE modeling for the semi-span wing model of the KARI SUAV

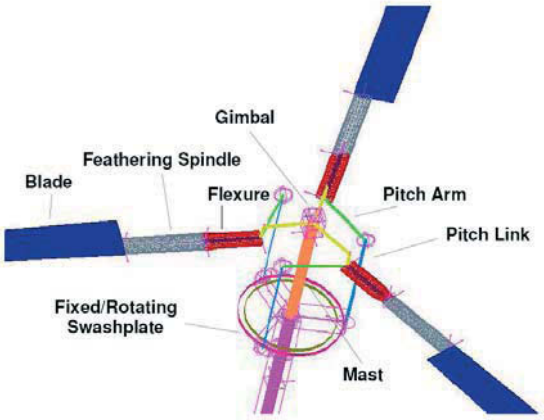

Figure 6 DYMORE modeling for the rotor system of the KARI SUAV

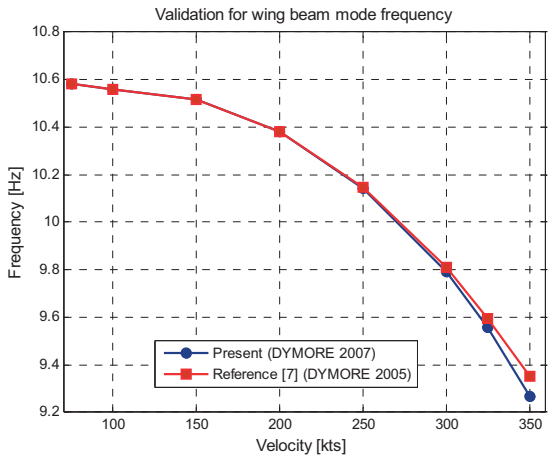

(a) Wing beam mode frequency

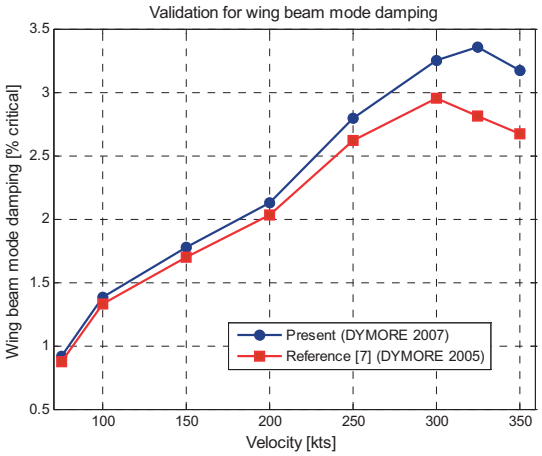

(b) Wing beam mode damping

Figure 7 Comparison of whirl flutter analysis results

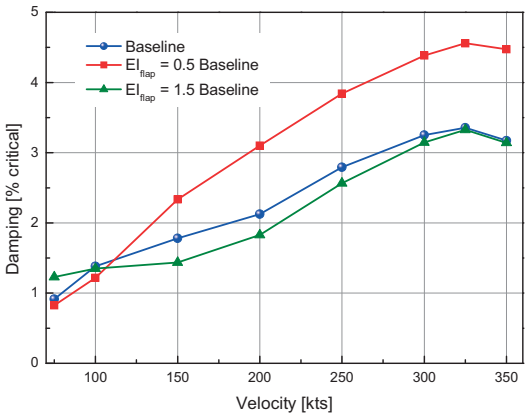

Figure 8 Variation of wing beam mode damping with wing flapwise bending stiffness
(airplane mode, Ω =1284 RPM)

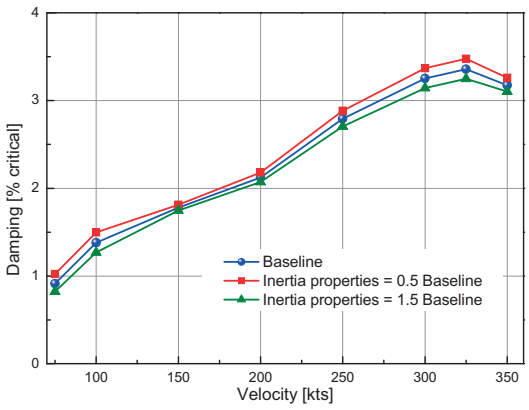

Figure 9 Variation of wing beam mode damping with wing inertial properties
(airplane mode, Ω =1284 RPM)

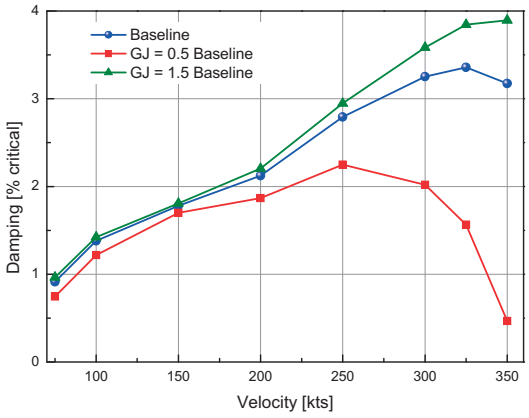

Figure 10 Variation of wing beam mode damping with wing torsional stiffness
(airplane mode, Ω =1284 RPM)

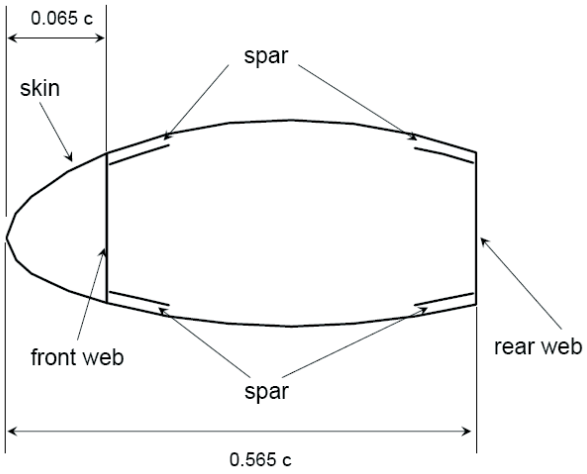

Figure 11 Cross-section model of a composite wing for design optimization studies

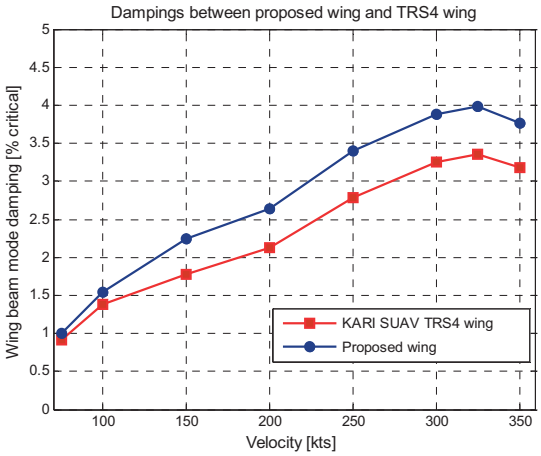

Figure 12 Comparison of whirl flutter stability of between two models with proposed wing and TRS4 wing (airplane mode, Ω=1284 RPM)

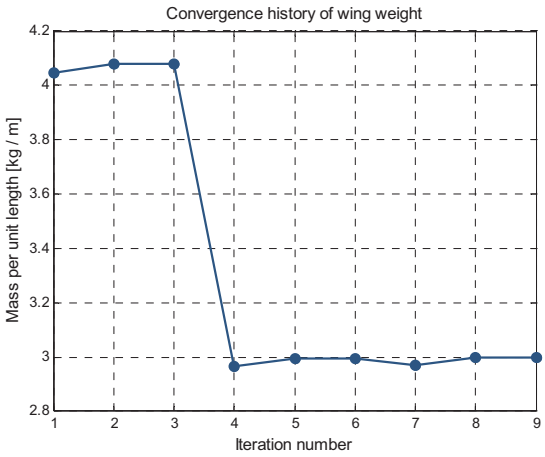

Figure 13 Convergence history of an objective function: the wing weight in Case 1

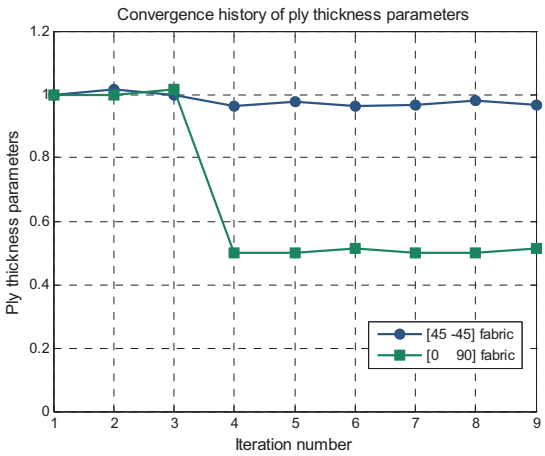

Figure 14 Convergence history of ply thickness parameters in Case 1

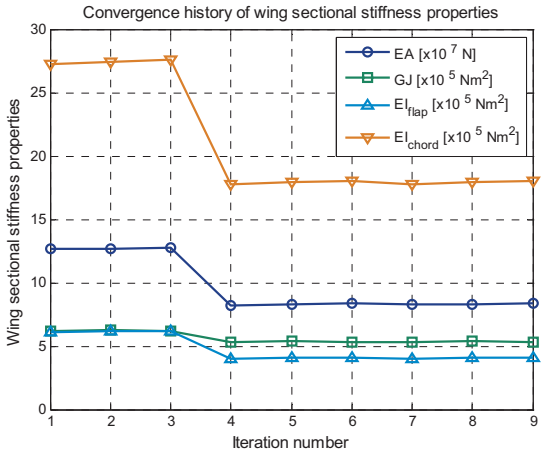

Figure 15 Convergence history of wing sectional stiffness properties in Case 1

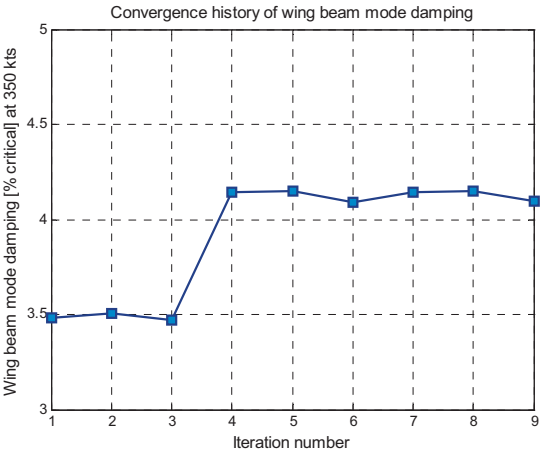

Figure 16 Convergence history of wing beam mode damping in Case 1

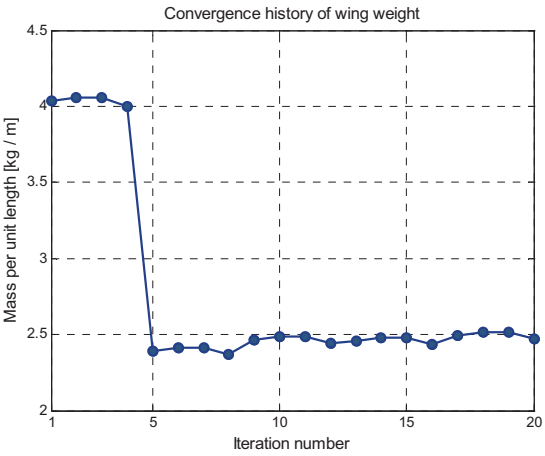

Figure 17 Convergence history of an objective function: the wing weight in Case 2

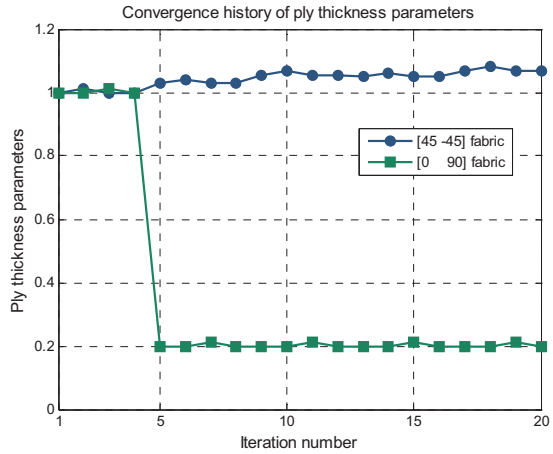

Figure 18 Convergence history of ply thickness parameters in Case 2

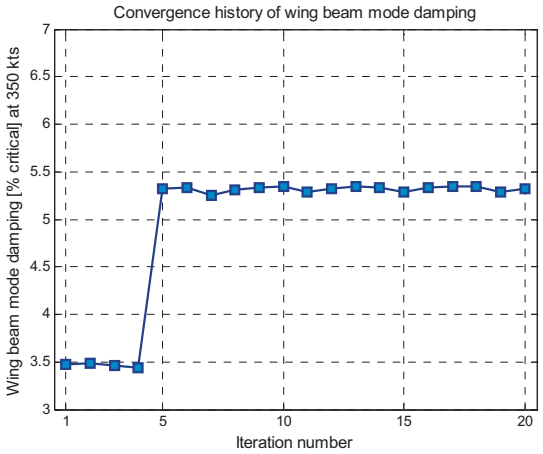

Figure 21 Convergence history of wing beam mode damping in Case 2

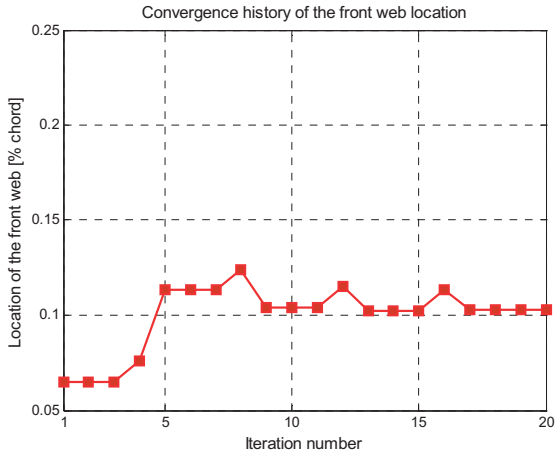

Figure 19 Convergence history of the front web location in Case 2

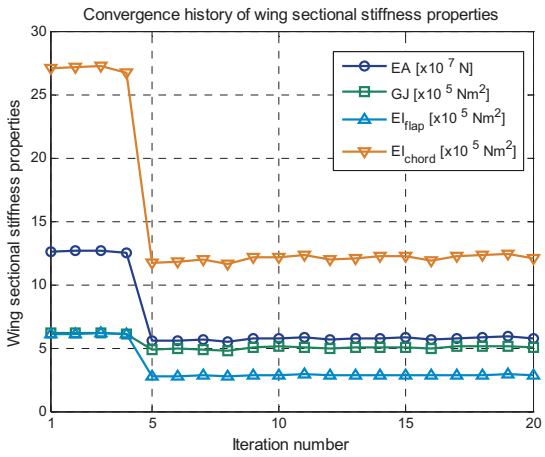

Figure 20 Convergence history of wing sectional stiffness properties in Case 2

Table 1 General properties of the KARI SUAV

Gross weight	907.2 kg (2000 lb)
Maximum speed	270 kts
Wing span length	6.8 m (22.3 ft)
Fuselage length	5 m (16.4 ft)
Rotor configuration	Gimbal
Number of blades	3
Rotor diameter	2.87 m (9.4 ft)
Rotor speed, Ω	1284 RPM (airplane mode) 1605 RPM (helicopter mode)

Table 2 Material properties of Carbon fabric

$E_1 = E_2$	58.16 GPa
G_{12}	8.72 GPa
ν_{12}	0.059
ρ	1460.9 kg/m^3
Ply thickness	0.000230 m

Table 3 Layup conditions for the skin and spar/web structures*

Skin	[45°-45°] [0°90°] [45°-45°] [0°90°]
Spar and web	[45°-45°] [0°90°] [45°-45°] [45°-45°] [0°90°] [45°-45°] [0°90°] [45°-45°] [0°90°]

* : Layup conditions are defined from the top to the bottom or from the outer to the inner

Table 4 Comparison of sectional stiffness between of proposed wing and at 75% span of the KARI TRS4 wing

Sectional stiffness	Proposed wing	TRS4 (at 75% span)	Difference (%)
EA [N]	1.339×10^8	1.449×10^8	-7.64
GJ [Nm^2]	7.038×10^5	6.253×10^5	12.53
EI_{flap} [Nm^2]	6.451×10^5	6.244×10^5	3.29
EI_{chord} [Nm^2]	2.891×10^6	3.063×10^6	-5.67

Table 5 Definition of an optimization problem in Case 1

Objective function	Wing weight (Mass per unit length) to be minimized	
Design variables	Ply thickness parameters t_k for [0 90] and [45 -45] fabrics	
Initial design values	All thickness parameters t_k are 1.0	
Design constraints	Center of gravity	0.22c ≤C.G.≤0.32
	Elastic axis	0.22c ≤E.A.≤0.32
	Ply thickness parameters	$0.5 \le t_k \le 2.5$
	Wing beam mode damping	Damping ≥ 0 at 350 kts
	Local strain in the worst loading case	Max. strain ≤ Ultimate strain of the constituent materials

Table 6 Definition of an optimization problem in Case 2

Objective function	Wing weight (Mass per unit length) to be minimized	
Design variables	- Ply thickness parameters t_k for [0 90] and [45 -45] fabrics - The front web location	
Initial design values	- All thickness parameters t_k are 1.0 - The front web location is 0.065c	
Design constraints	Center of gravity	0.22c ≤C.G.≤0.32
	Elastic axis	0.22c ≤E.A.≤0.32
	Ply thickness parameters	$0.2 \le t_k \le 2.5$
	Front web location	$0.06 \le web_{loc} \le 0.37$
	Wing beam mode damping	Damping ≥ 0 at 350 kts
	Local strain in the worst loading case:	Max. strain ≤ Ultimate strain of the constituent materials